

Critical sheet resistance observed in high- T_c oxide-superconductor $\text{Nd}_{2-x}\text{Ce}_x\text{CuO}_4$ thin films

Satoshi Tanda, Minoru Honma, and Tsuneyoshi Nakayama
Department of Applied Physics, Hokkaido University, Sapporo 060, Japan
 (Received 7 December 1990)

High- T_c oxide-superconductor $\text{Nd}_{2-x}\text{Ce}_x\text{CuO}_4$ single-crystal thin films were used to observe the critical sheet resistance at the insulator-superconductor transition. The films were epitaxially grown on $\text{SrTiO}_3(100)$ by the method of molecular-beam epitaxy. The electron transport properties of these films are drastically influenced by oxygen-impurity concentration and show clearly the evidence of Anderson localization attributed to two dimensionality. It is found that the critical sheet resistance R_\square at the onset of superconductivity takes a value within a range from 6 to 8 $\text{k}\Omega$, which is close to the value $h/4e^2 = 6.45 \text{ k}\Omega$. Our results provide clear evidence that Anderson localization induces the universal behavior observed at the superconductor-insulator transition.

Recently there has been considerable interest in the physical origin of the insulator-superconductor transition in disordered thin films at very low temperatures.¹⁻⁶ One of the reasons for this interest is the observation that the onset of superconductivity appears to occur when the normal-state sheet resistance R_\square falls below a critical value close to $h/4e^2 = 6.45 \text{ k}\Omega$, between superconductivity and electron localization in a disordered two-dimensional (2D) system; this critical value may be universal, independent of materials and microscopic structures. Granular thin films¹⁻⁴ or homogeneous ultrathin films^{5,6} have been used to observe the critical sheet resistance R_\square , since the superconducting transition temperature T_c can be suppressed to very low values by changing the sizes of the grains or film thickness. The ultrathin films of high-temperature oxide superconductors have been also used to observe the critical sheet resistance.^{7,8}

In this paper, we report measurements of the critical normal sheet resistance R_\square using oxide-superconductor $\text{Nd}_{2-x}\text{Ce}_x\text{CuO}_4$ single-crystal thin films prepared by the method of molecular-beam epitaxy (MBE). It is found that the critical sheet resistance R_\square takes a value between 6 and 8 $\text{k}\Omega$. Our measurements were made by varying gradually the oxygen contamination in single-crystal thin films by heat treatment. This is quite different from earlier reports for ultrathin amorphous films or granular thin films. We discuss the relation between earlier reports and our results for the thin films of oxide superconductor $\text{Nd}_{2-x}\text{Ce}_x\text{CuO}_4$.

$\text{Nd}_{2-x}\text{Ce}_x\text{CuO}_4$ single-crystal films (5 mm \times 5 mm \times 1000 \AA , $x=0.15-0.20$) were grown on $\text{SrTiO}_3(100)$ by the method of MBE using Knudsen cell sources for Nd, Cu, and Ce. Oxygen pressure partial was 10^{-4} Torr in the processing chamber. The details of our MBE method will be reported elsewhere. The crystal structures of the films were characterized by x-ray-diffraction analysis. The appearance of only (002n) sharp peaks indicates that the (001) plane is highly oriented parallel to the film surface, i.e., that the films were grown epitaxially on $\text{SrTiO}_3(100)$. The lattice constant c was derived from the reflection signals: $c = 12.07 \text{ \AA}$ ($x=0.15$) and $c = 12.06 \text{ \AA}$ ($x=0.18$), close to those of $\text{Nd}_{2-x}\text{Ce}_x\text{CuO}_4$ ceramics.⁹ The film thickness, determined from the cross section of the films by the electron microscope, was 1000 \AA within

an accuracy of a few percent.

In order to obtain excessively oxidized samples, the films were heated up to 950 $^\circ\text{C}$ in air and kept at that temperature for 120 min, and quenched down to room temperature. These oxidized films were reduced in Ar (pressure 0.4 Torr, with O_2 pressure of less than 10^{-6} Torr) at temperatures ranging from 500 to 700 $^\circ\text{C}$ for 20 min. This annealing in vacuum plays a role in reducing the oxygen concentration in $\text{Nd}_{2-x}\text{Ce}_x\text{CuO}_4$ films, which is required for the appearance of the superconductivity. We have measured the resistivities down to liquid-He temperature at various stages of oxygen reduction, and find that the films show the insulator-superconductor transition under some conditions of oxygen contamination.

The temperature dependences of resistivities $\rho(T)$ were measured by the standard four-terminal method with evaporated gold electrodes. The current terminals were covered with gold electrodes along the edge of the films in order to eliminate the ambiguity due to inhomogeneous current flow arising from strong anisotropy. The current density was taken as 10 A/cm^2 throughout our measurements. The sheet resistances R_\square per CuO_2 layer were obtained using the relation $R_\square = \rho/d$, where $d (=6.03 \text{ \AA})$ is the lattice spacing between CuO_2 layers in $\text{Nd}_{2-x}\text{Ce}_x\text{CuO}_4$ film ($x=0.18$). This relation is based on the assumption that each CuO_2 layer forms a two-dimensional superconducting sheet. The assumption is reasonable because the resistivities along the basal plane ρ_{ab} and along the c axis ρ_c are highly anisotropic, with a ratio that becomes ~ 1000 .¹⁰ In addition, the validity of the assumption will become clear from our confirmation that the normal-states transport properties of the films show the typical characteristics of weak localization associated with two dimensionality (see Figs. 2 and 3). The sheet resistances R_\square for $\text{Nd}_{2-x}\text{Ce}_x\text{CuO}_4$ films are plotted in Fig. 1 as a function of temperature for two samples ($x=0.18$, A-E; 0.16, F) in which oxygen impurities were reduced by the procedure mentioned above. We emphasize here that the curves A-E are the data taken from the same sample but with different oxygen contamination. The point is that the insulator-superconductor transition was observed using the same single-crystal film. Detailed discussion of the data will be given later.

Figure 2 shows the measurements of magnetoresis-

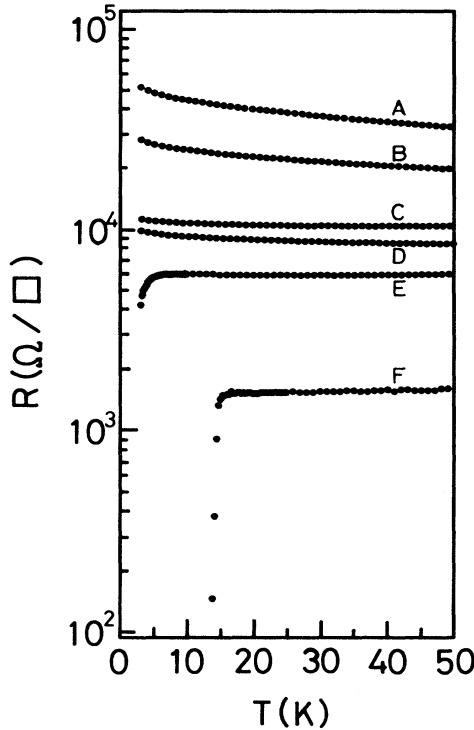


FIG. 1. Temperature dependence of the sheet resistance R_{\square} for $\text{Nd}_{2-x}\text{Ce}_x\text{CuO}_{4+y}$ single-crystal films. The curves A–E are for $x=0.18$, and F for $x=0.16$. From A to E, excess oxygen concentration y is varied by changing the annealing conditions: A at 500°C , B at 550°C , C at 600°C , D at 650°C , and E at 700°C , respectively, for 20 min in a vacuum ambient (Ar pressure of 0.4 Torr and O_2 pressure of less than 10^{-6} Torr). Curve F shows the data with high transition temperature T_c in a series of our experiments.

tances at temperature $T=4.2$ K as a function of magnetic field H : $[\Delta R(H)/R(0)] = [-\Delta\sigma(H)R(0)]$ for the sample $x=0.18$ (from the curve B plotted in Fig. 1), where $\Delta R(H) = R(H) - R(0)$. The dotted points in Fig. 2 are the experimental data for the magnetic fields applied perpendicularly to the film surface. These data clearly exhibit negative resistance with increasing magnetic fields, that is, the data in Fig. 2 indicate that the magnetoresistance decreases with increasing magnetic fields, following a

$$\Delta\sigma(H) = \sigma(H) - \sigma(0) = \frac{-ae^2}{2\pi^2\hbar} \left[\psi \left(\frac{1}{2} + \frac{1}{a\tau} \right) - \psi \left(\frac{1}{2} + \frac{1}{a\tau_\varepsilon} \right) - \ln \left(\frac{\tau_\varepsilon}{\tau} \right) \right]. \quad (1)$$

Here a is the constant prefactor, τ the relaxation time due to normal impurity scattering, τ_ε the inelastic scattering time, and $a=4DeH/\hbar$ where D is the diffusion coefficient. This formula was derived under the condition $a\tau < 1$, where $a\tau = 4e_F\omega_c\tau^2/\hbar$. The solid curve in Fig. 2 was determined using Eq. (1) from least-squares fitting. Best fitting were obtained by choosing $\tau/\tau_\varepsilon=0.05$ and $a\tau_\varepsilon=15$, respectively. Thus, we see that formula (1) is applicable for our case because $a\tau=0.75$.

Now let us return to the discussion on the experimental data given in Fig. 1. As seen from the curves (D and E)

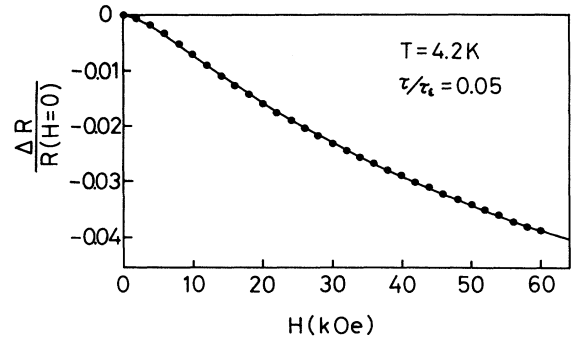


FIG. 2. Magnetic-field dependence of resistance $\Delta R(H)/R(H=0)$ at $T=4.2$ K, in which magnetic fields H are applied normally to the film surface. These data are obtained from the sample corresponding to curve B in Fig. 1. The experimental points are fitted to expression (1) using the values of parameters given in the text.

quadratic form H^2 at weak magnetic fields, and a logarithmic one above $H=20$ kOe. We have also confirmed the logarithmic temperature dependence of the resistance, though this is omitted here.

Figure 3 shows the dependence of the magnetoresistance on the angle to the film surface at temperatures 4.2 K and at constant field $H=60$ kOe. A typical oscillating characteristics originating in the two dimensionality is found from the data given in Fig 3, as in the case of a two-dimensional Si-metal-oxide-semiconductor inversion layer.¹¹ All of these data give us evidence that our system is in the weakly localized regime (WLR) and really two dimensional.

In the weakly localized regime, quantum interference causes spatially localized states which produce a quantum correction to the classical Drude conductivity σ_0 . This weak-localization correction is sensitive to perturbations which destroy time-reversal symmetry. This suggests that a magnetic field suppresses the quantum interference effect and gives rise to negative magnetoresistance. Following this idea, numerous theories have been proposed to interpret the magnetic-field dependence of the conductivities.^{12,13} The change in conductivity with magnetic field H applied perpendicularly to the 2D plane is expressed in terms of the digamma function $\psi(z)$,¹⁴

in Fig. 1, the change from the insulating state (R_{\square} increase as $T \rightarrow 0$) to the superconducting state (R_{\square} decrease as $T \rightarrow 0$) occurs between 6 and 8 kΩ, close to a value $\hbar/4e^2=6.45$ kΩ. Whether or not the $R_{\square}(T)$ data fall to zero just after this transition is not possible to resolve by the present measurements which were limited to a range of temperatures above 4.2 K.

Our observations of the superconductor-insulator transition naturally indicate that the phenomenon is related to the competition between electron localization and superconductivity. There are two length scales characterizing

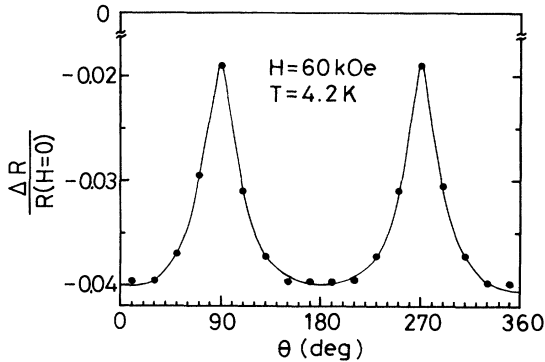


FIG. 3. Angular dependence of the transverse magnetoresistance for the normalized negative part $\Delta R(H)/R(H=0)$ for curve B in Fig. 1 at $H=60$ kOe and $T=4.2$ K, where $\theta=0^\circ$ at $H \perp$ surface. The solid curve is only a guide for the eye.

our systems. These are the superconducting coherence length ξ and the electron localization length l_e due to the random distribution of impurities (oxygen in our case): $l_e \approx l \exp(\pi k_F l / 2)$, where l is the mean free path. In our system the latter can be regarded as the control parameter for the onset of superconductivity. We can estimate the order of the mean free path l as follows: It is believed that oxygen impurities are a key element for electron localization for $\text{Nd}_{2-x}\text{Ce}_x\text{CuO}_4$, in which excess oxygen impurities are reduced by heat treatment. These excess oxygen impurities occupy different sites from those at the superconducting CuO_2 layer and play a role as impurity potentials. Though the definite position of excess oxygen impurities is not crucial in the present work, the reasonable positions seem to be those as close as possible to CuO_2 layers. It is known that the largest value of excess oxygen concentration is around $y=0.04$ ($\text{Nd}_{2-x}\text{Ce}_x\text{CuO}_{4+y}$).¹⁵ From this value, we can estimate the smallest mean free path due to elastic scattering as $l \sim 20$ Å, where use is made of the relation $a^2/l^2=0.04$, and the lattice constant is taken as $a=3.95$ Å. As oxygen impurities are reduced by heat treatment, the mean free path l increases, i.e., the localization length l_e increases exponentially and crosses over the coherence length $\xi(T)$ at some value of oxygen concentration. It is natural to claim that, when l_e is smaller than the average size of a Cooper pair (ξ), the electrons exist as localized states and the pairs are broken due to the effect of Coulomb repulsion and vice versa. Thus the criterion for the onset of superconducting state is $l_e \approx \xi$.¹⁶ It should be noted that the effect of disorder on superconductivity has been intensively discussed in connection with Anderson localization by Maekawa and Fukuyama.¹⁷

In the case of ultrathin films, the length scale l is the average size of the superconducting grains. When the size

of grains is larger than $\xi_0/(k_F l)^{1/2}$, the system is viewed as consisting of randomly coupled Josephson junctions, where each grain is described by a single order parameter. Most experiments for granular thin films reported so far¹⁻⁴ utilize the fact that the grain sizes can be artificially varied by choosing the appropriate deposition condition.

To summarize, we have observed the critical sheet resistance using oxide-superconductor $\text{Nd}_{2-x}\text{Ce}_x\text{CuO}_4$ films, which were epitaxially grown on $\text{SrTiO}_3(100)$ by the MBE method. Thermal treatment of films gradually reduced the oxygen-impurity concentration and resulted in the appearance of the superconducting state. It is remarkable that our system with high impurity density shows clear evidence of Anderson localization originating in two dimensionality. Oxide-superconductor $\text{Nd}_{2-x}\text{Ce}_x\text{CuO}_4$ thin films are particularly advantageous for the observation of the critical sheet resistance, because these have two-dimensional CuO_2 superconducting layers and the impurity (oxygen) density can be continuously varied by heat treatment. This implies that one can set up the situation where the localization length l_e crosses over the coherence length ξ , i.e., the control parameter for the onset of superconductivity is the oxygen concentration. There are a variety of theories to explain the critical sheet resistance observed at the onset of superconductivity.¹⁸⁻²⁴ Among them, the theories assuming Josephson coupling between superconducting islands will be ruled out because such a picture is not appropriate for our system. It seems to be necessary to develop the theory from very general points of view incorporating explicitly the aspect of Anderson localization to explain our observation.^{21-23,25}

We conclude that our findings for oxide-superconductor $\text{Nd}_{2-x}\text{Ce}_x\text{CuO}_4$ films provide an interesting system for revealing the mechanism for the superconductor-insulator transition. In particular, we have presented clear evidence that Anderson localization induces the universal behavior observed at the insulator-superconductor transition. Another important feature is that our results play a role in investigating the nature of electron pairing or the normal-state properties of high- T_c oxide superconductors.

The authors would like to thank N. Hatakenaka, NTT Basic Research Laboratory, for stimulating discussions, and I. Aoyama of Komatsu Ltd. Material Research Laboratory for experimental supports. They are also grateful to T. Sambongi, K. Yamaya, and T. Honma, who assisted them with the use of high-magnetic-field facilities. They are indebted to K. Yakubo and A. Ohi for useful discussions, and Y. Nishida for experimental support at the early stage of this work. Finally, Hiroshi Takahashi of Eiko Engineering Company should be thanked, whose support made our experiments possible.

¹B. G. Orr, H. M. Jaeger, and A. M. Goldman, Phys. Rev. B **32**, 7586 (1985); B. G. Orr *et al.*, Phys. Rev. Lett. **56**, 378 (1986); H. M. Jaeger *et al.*, Phys. Rev. B **34**, 4920 (1986); H. M. Jaeger *et al.*, *ibid.* **40**, 182 (1989).

²L. J. Geerlings and J. E. Mooij, Physica B **152**, 212 (1988).

³S. Kobayashi, Physica B **152**, 223 (1988).

⁴A. Gerber, J. Phys. Condens. Matter **2**, 8161 (1990).

⁵D. B. Haviland *et al.*, Phys. Rev. Lett. **62**, 2180 (1989), D. B. Haviland *et al.*, Physica B **165** & **166**, 1457 (1990).

⁶A. F. Hebbard and M. A. Paalanen, Phys. Rev. Lett. **65**, 927

- (1990).
- ⁷N. Nishida, *Solid Stat Phys. (Tokyo)*, **25**, 874 (1990).
- ⁸T. Wang *et al.*, *Physica B* **165 & 166**, 1463 (1990).
- ⁹A. Hebbard *et al.* (unpublished).
- ¹⁰Y. Hidaka and M. Suzuki, *Nature (London)* **338**, 635 (1989).
- ¹¹As a review, see, for example, S. Kawaji, in *Symposium on Recent Topics in Semiconductor Physics*, edited by H. Kamimura and Y. Toyozawa (World Scientific, Singapore, 1983), p. 165.
- ¹²For a review, see, for example, P. A. Lee and T. V. Ramakrishnan, *Rev. Mod. Phys.* **57**, 287 (1985).
- ¹³For a review, see, for example, H. Fukuyama, in *Modern Problems in Condensed Matter Sciences*, edited by A. L. Efros and M. Pollack (North-Holland, Amsterdam, 1985), Vol. 10, p. 155; B. L. Altschuler and A. G. Arnov, *ibid.*, p. 1.
- ¹⁴S. Hikami, A. I. Larkin, and Y. Nagaoka, *Prog. Theor. Phys.* **63**, 807 (1980).
- ¹⁵Y. Tokura, H. Takagi, and S. Uchida, *Nature (London)* **337**, 345 (1989).
- ¹⁶M. Ma and P. A. Lee, *Phys. Rev. B* **35**, 1459 (1985).
- ¹⁷S. Maekawa and H. Fukuyama, *J. Phys. Soc. Jpn.* **51**, 1380 (1982).
- ¹⁸S. Chakravarty *et al.*, *Phys. Rev. Lett.* **56**, 2203 (1986).
- ¹⁹S. Chakravarty *et al.*, *Phys. Rev. B* **35**, 7256 (1986).
- ²⁰R. A. Ferrel and B. Mirkashem, *Phys. Rev. B* **37**, 648 (1988).
- ²¹T. Pang, *Phys. Rev. Lett.* **62**, 2176 (1989).
- ²²M. P. A. Fisher and D. H. Lee, *Phys. Rev. B* **39**, 2756 (1989); D. H. Lee and M. P. A. Fisher, *Phys. Rev. Lett.* **63**, 903 (1989).
- ²³M. P. A. Fisher, *Phys. Rev. Lett.* **65**, 923 (1990).
- ²⁴A. Gold, *Z. Phys. B* **81**, 155 (1990).
- ²⁵T. V. Ramakrishnan, in *Chance and Matter*, edited by J. Souletie, J. Vannimenus, and R. Stora (North-Holland, Amsterdam, 1987), p. 213.